Proceedings World Geothermal Congress 2015
Melbourne, Australia, 19-25 April 2015

The Performance of Compression-absorption Heat Pump System Using Low-temperature Geothermal Tail Water

Yulie Gong, Chao Luo, Yuan Yao, Zhenneng Lu, Weibin Ma

Guangzhou Institute of Energy Conversion, Chinese Academy of Sciences, Guangzhou 510640, Guangdong, China

Key Laboratory of Renewable Energy, Chinese Academy of Sciences, Guangzhou 510640, Guangdong, China

Email: gongyl@ms.giec.ac.cn

Keywords: CAHP; COP; vertical out-tube falling film; generator; ammonia-water

ABSTRACT

In China the resources of low-temperature geothermal water between 20 to 40 ℃ are very rich, and there are also a lot of geothermal tail water and waste heat water, which are discharged with the similar temperature. In order to reduce the energy consumption of building district heating, heat pump is often used to recover low-temperature geothermal tail water. Among the heat pump technologies, the compression-absorption heat pump (CAHP) has been recognized for a long time. Comparing with the compression heat pump, CAHP can get a high heat sink temperature with a lower compression ratio, and the temperature glide of the generator and absorber in CAHP can be fitted to the heat source and heat sink, which lead to a higher COP.

The performance of a CAHP system using the ammonia-water mixture is analyzed in this paper. A model based on mass and energy balances in all components is developed, and a model of the vertical out-tube falling film generator is conducted especially. The results show that there is an optimum concentration around 65% for the system. The maximum overall heat transfer coefficient can be obtained with the optimum spray density of around 0.16 kg · m^{-1} · s^{-1}. Based on a high heat sink temperature of 65℃ and a low heat source temperature from 30 to 40℃, the COP of the CAHP system is above 4.

1. INTRODUCTION

In China the low-temperature geothermal heat water below 50℃ is plentiful, and there is also a lot of geothermal tail water and residual heat water which is discharged with the same temperature. On the other hand, the energy consumption for heating is tremendous. It will be meaningful for us to recover the residual heat efficiently to supply heating, Heat pump is an efficient technology to reduce energy consumption, which can recover low-temperature residual heat and meet the demand for heating water if designed reasonably. Among the heat pump technologies, the potential of the CAHP cycle has been recognized for a long time (Bourouis et al., 2000). Comparing with the traditional compression heat pump, CAHP can get a high heat sink temperature with a lower compression ratio (Ventas et al., 2010; Hulten and Berntsson 1999), and the generator and absorber temperature glide can be fitted to gliding temperatures of the heat source and heat sink, which leading to a higher COP (Stokar and Trepp 1986). In addition, the system can be operated efficiently with low-temperature water (Fukuta et al., 2002). Several earlier studies showed that the heat transfer coefficient of the generator in the test plant influences the COP and other state variables, and the COP increases sharply with improving heat transfer of generator (Stokar, 1987; Rameshkumar et al., 2009). However, there is no ideal design practice for the CAHP generator so far. So, it is necessary to develop a new simulation model to optimize the generator. The advantages of vertical falling-film heat transfer are widely recognized in the past studies (Chun and Seban, 1971; Stokar and Trepp, 1986; Hulten and Berntsson, 2002), but the low-temperature heat source condition was very infrequent. Therefore, in the present study, a new model of the CAHP system with a vertical out-tube falling film generator is developed.

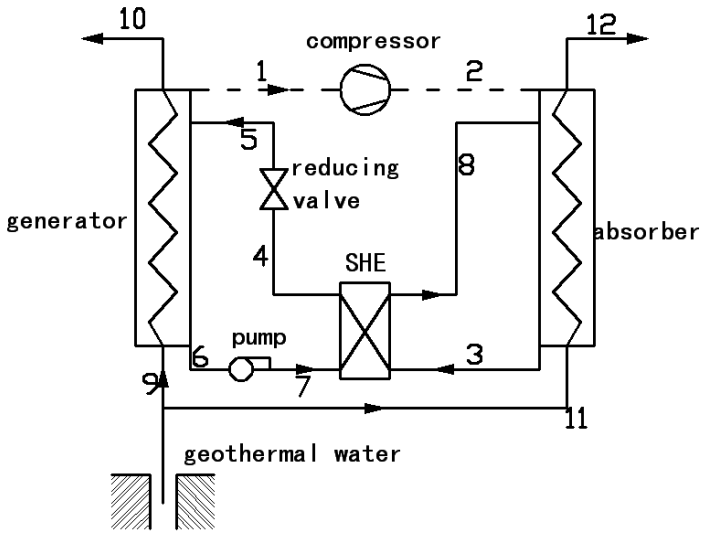

Fig. 1 Schematic diagram of CAHP system

2. SYSTEM DESCRIPTION AND ANALYSIS

2.1 System description

The CAHP cycle includes a compression stage and an absorption stage. The compressor raises the gases which desorbed from the generator to a high pressure and then the gases enter into the absorber where contact with the weak solution. In the absorber, the gases are absorbed by the weak solution, and the absorption heat is released to the heat sink. After that the rich solution preheats the weak solution in the solution heat exchanger (SHE) and passes through the reducing valve and then enters the generator again.

2.2 System analysis

In several earlier studies (Eckhard, 1997), the ammonia-water mixture was the most interesting working fluid because of the excellent properties of ammonia and the large experience handling in industrial applications, therefore ammonia is also chosen for the present study. Moreover, the composition change in the CAHP system has a substantial influence on the COP (Satapathy, 2008) and the former research showed that the optimal design of generator is essential (Tyagi et al., 2010). In order to establish the optimum operating conditions of the cycle, different concentration of solution, cycle ratios, heat source temperature, spray density of the generator are performed in sensitivity studies. The simulation of the CAHP cycle is based on energy balances for the internal stream and external stream. The properties of fluid at inlet and outlet are expressed in terms of temperature, pressure, concentration and enthalpy.

3. METHODOLOGY

3.1 Generator simulation

The schematic of the generator is represented in Fig. 2. The generator is a single-pass counter current vertical out-tube falling film heat exchanger with the solution outside the smooth tubes and the geothermal water inside the tubes.

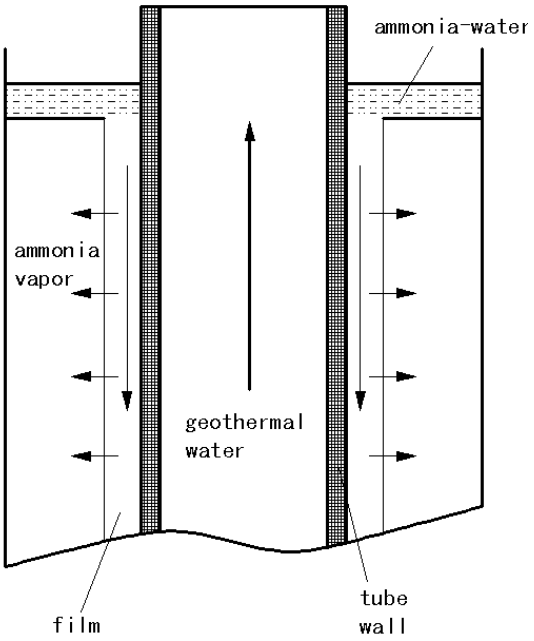

Fig. 2 Schematic diagram of a vertical out-tube falling film generator

In order to simplify the mathematical model, the following assumptions are made:

1) The heat transfer between the wall and geothermal water obeys to the first boundary condition;

2) Heat conductivity in the direction of flow is negligible;

3) The fluid outside the tube is regarded as Newtonian fluid and unsteady;

4) Mass transfer resistance is negligible;

5) Fluid is ideally mixed in the direction perpendicular to the flow;

6) There is no interaction force between the liquid and vapor;

7) There is no heat transfer between the liquid and vapor except evaporation heat.

3.2 Generator boundary conditions

The governing equations are given as follows:

Continuity equation $$\frac{\partial (\rho U)}{\partial x}+\frac{\partial(\rho V)}{\partial \mathrm{y}}=0 \quad (1)$$

Momentum equation $$\rho U\frac{\partial U}{\partial x}+\rho V\frac{\partial U}{\partial y}=\frac{\partial}{\partial y}\left(\mu\frac{\partial U}{\partial y}\right)+\rho g \tag{2}$$

Energy equation $$\rho C_p U\frac{\partial T}{\partial x}+\rho C_p V\frac{\partial T}{\partial y}=\frac{\partial}{\partial y}\left(\lambda\frac{\partial T}{\partial y}\right) \tag{3}$$

Mass conservation equation $$\rho \mathrm{U}\frac{\partial \xi}{\partial x}+\rho V\frac{\partial \xi}{\partial y}=\frac{\partial}{\partial y}\left(\rho D_m\frac{\partial \xi}{\partial y}\right) \tag{4}$$

The boundary conditions are given as follows:

1) Entrance boundary conditions

$$\delta\big|_{x=0}=\delta_0 \tag{5}$$

$$V\big|_{x=0}=0 \tag{6}$$

$$T\big|_{x=0}=T_0 \tag{7}$$

$$\xi\big|_{x=0}=\xi_0 \tag{8}$$

$$\mathrm{U}\,|_{\mathrm{X}=0}=\frac{\Gamma}{\rho\delta_0}|\mathrm{x}=0 \tag{9}$$

2) No slip boundary condition

$$U\big|_{y=0}=V\big|_{y=0} \tag{10}$$

3) Non-filtration boundary conditions

$$\frac{\partial \xi}{\partial \mathrm{y}}|_{\mathrm{y}=0}=0 \tag{11}$$

$$T\big|_{y=0}=T_0 \tag{12}$$

4) Boundary conditions of liquid-vapor interface

$$\lambda\frac{\partial \mathrm{T}}{\partial \mathrm{y}}|_{y=\delta}=-\Delta H\frac{\rho D_m}{\xi}\frac{\partial \xi}{\partial y} \tag{13}$$

$$\frac{\partial U}{\partial y}|_{y=o}=0 \tag{14}$$

$$F\left(P_g,T_f,C_f\right)\big|_{y=\delta}=0 \tag{15}$$

$$\left(\rho V+\rho U\frac{d\delta}{dx}\right)|_{y=\delta}=-\frac{\rho D_m}{\xi}\frac{\partial \xi}{\partial y}|_{y=\delta} \tag{16}$$

The flow rate, solution concentration and temperature can be calculated by the above mathematical model.

Table 1 Inputs of the generator model

Variable	Value	Variable	Value
δ	2mm	V_w	100-500L/h
height	5m	P	0.2-2MPa
D_i	21mm	v	0
D_o	25mm	Γ	0.06-0.26 kg·m-1·s-1
ξ	55%-70%	T_9	30-40℃

3.3 Cycle simulation

The system analysis is carried out for heating applications with the following assumptions:

1) The system is working under steady-state conditions;

2) The processes in absorber and generator are considered adiabatic, and the process in the reducing valve is isenthalpic;

3) The weak solution at the exit of the generator and the strong solution at the exit of absorber are saturated;

4) The effect of pressure drops in various components on the system performance was assumed to be negligible;

5) Due to the large difference between the boiling points of water and ammonia, the concentration of the vapor is considered as 99.8%.

The correlations proposed by Xu (1995) were used to calculate the thermodynamic properties of the saturated solution and vapor. Chemical equilibrium was assumed at the exit of each component.

3.4 Energy balance

The energy balance across the components is shown as follows:

Generator

$$Q_{\mathrm{gw}} + m_5 h_5 = m_6 h_6 + m_1 h_1 \tag{16}$$

$$Q_{gw} = m_{gw}\left(h_9 - h_{10}\right) = m_{gw} k_g \cdot A_g \cdot \Delta T_g \tag{17}$$

$$m_6 + m_1 = m_5 \tag{18}$$

Compressor

$$W_c = m_1\left(h_2 - h_1\right)/\eta_{is} \tag{19}$$

Absorber

$$Q_a + m_3 h_3 = m_8 h_8 + m_1 h_2 \tag{20}$$

$$m_3 = m_8 + m_1 \tag{21}$$

$$Q_a = m_{aw}\left(h_{12} - h_{11}\right) = m_{aw} \cdot k_a \cdot A_a \cdot \Delta T_a \tag{22}$$

Pump

$$W_p = m_6\left(h_7 - h_6\right)/\eta_p \tag{23}$$

Compression ratio

$$\varepsilon = p_2 / p_1 \tag{24}$$

At each pressure ratio, according to a screw compressor cooled with an insoluble oil, the isentropic efficiency data used are as follows (Hulten and Berntsson, 1999):

$$\eta_{is} = -0.143 + 0.55\varepsilon - 0.0867\varepsilon^2 \quad \text{for } \varepsilon = 2 \sim 3.5 \tag{25}$$

$$\eta_{is} = -0.766 + 0.0131\varepsilon \quad \text{for } \varepsilon = 3.5 \sim 10 \tag{26}$$

$$COP = Q_a / \left(W_c + W_p\right) \tag{27}$$

In this study, *COP* corresponds to the efficiency of the machine on Power consumption basis. The compression ratio of the system is calculated based on the simulation. In order to analyze the system performance, the heat source temperature and the solution concentration are chosen as input variables.

4. RESULTS AND DISCUSSION

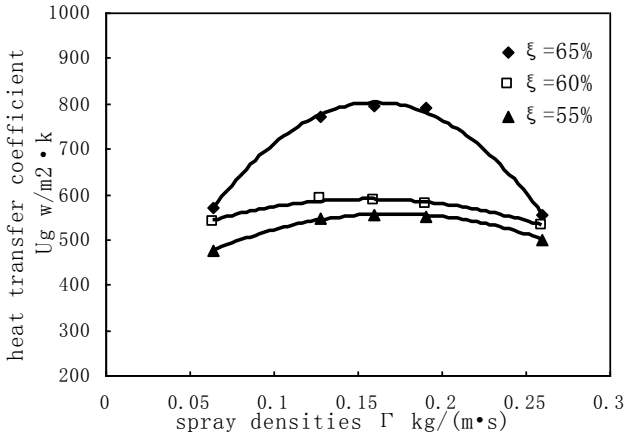

Fig. 3 U_g- Γ relationship with different strong solution concentration (geothermal water temperature T_9=30℃， volume flow V_g=500L/h)

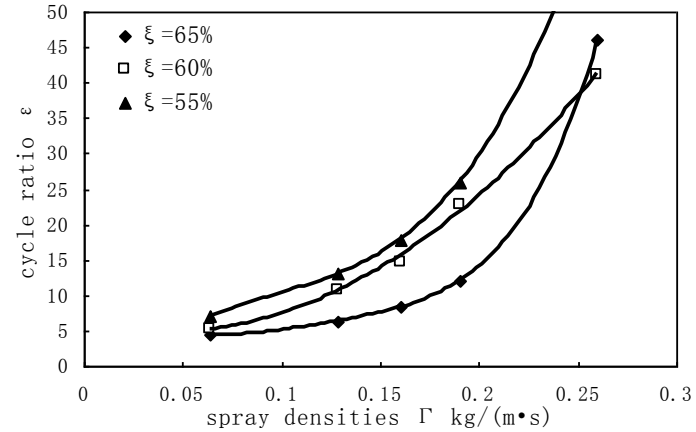

Fig. 4 ε - Γ relationship with different strong solution concentration (geothermal water temperature T_9=30℃， volume flow V_g =500L/h)

Fig.3 shows the overall heat transfer coefficient U_g changes along with the inlet spray density Γ. When the water temperature and volume flow are constant, all curves show that the U_g firstly increases and decreases later with increasing Γ. This occurs because larger spray density bring higher velocity of film flow, which will be conducive to heat transfer, however, when spray density exceed the optimum value the film will became thickness, and the heat transfer resistance increases. Fig 4 shows the compression ratio ε increases when spray density increases, but it increases gently when the Γ less than 0.2 $kg \cdot m^{-1} \cdot s^{-1}$, which means increasing spray density will result in higher power consumption of the compressor. From fig.3 and fig.4, the spry density has a positive effect on the system performance, and there is an optimum value of spry density, in this case it is around 0.15 $kg \cdot m^{-1} \cdot s^{-1}$.

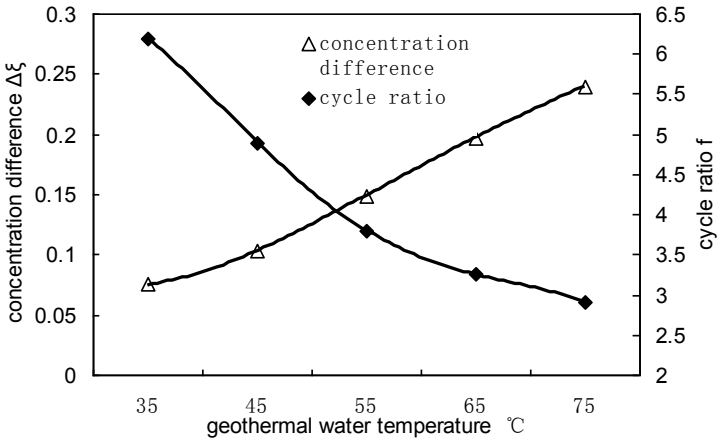

Fig. 5 The effect of geothermal water temperature on concentration difference and cycle ratio (spray density Γ=0.13 $kg \cdot m^{-1} \cdot s^{-1}$, geothermal water V_g =500L/h, strong solution concentration ξ=65%)

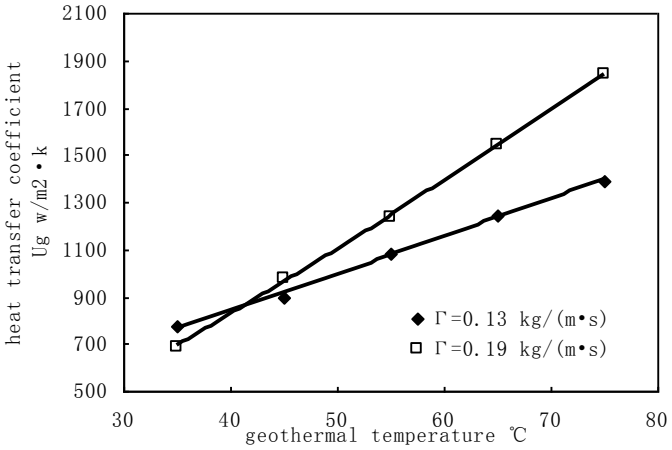

Fig. 6 The changes of U_g along with geothermal water temperature at different spray densities (geothermal water V_g =500L/h, strong solution concentration ξ=65%)

It can be seen from Fig. 5 that the heat source temperature has significant impact on the concentration difference and cycle ratio. In the CAHP system the cycle ratio has a large effect on *COP* (Rameshkumar et al., 2009), which means the heat source temperature also makes a big difference on *COP*. When the concentration is 65%, a high concentration difference about 10% can be obtained. Fig. 6 shows that when the heat source temperature increases, the U_g increase linearly. At the same condition, when the temperature is blow 40℃, the value of U_g at different spray densities is close, which is correspond to the generator experimental research of Stokar and Trepp (1986), it also indicates that the further study about vertical out-tube falling film heat transfer at the low-temperature condition is necessary.

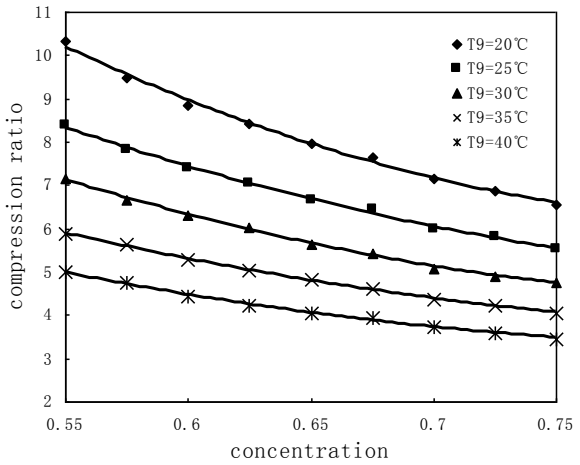

Fig. 7 The changes of ε along with concentration at different heat source temperatures (heat sink temperature T_{12}=65℃)

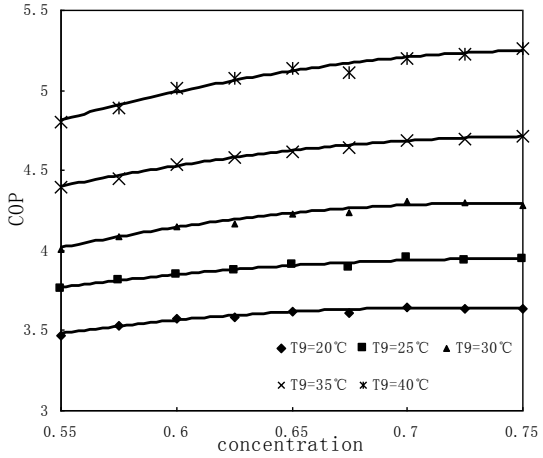

Fig. 8 The changes of *COP* along with concentration at different heat source temperatures (heat sink temperature T_{12}=65℃)

Fig. 7 shows that for different geothermal water inlet temperatures (T_9) compression ratio ε decreasing as the concentration increases. The changes of concentration have great influence on the value of compression ratio. The *COP* changes along with the

variation of T_9 shown in Fig. 8. Each curve shows the *COP* as a function of concentration, and at the same concentration, *COP* is larger for higher heat source temperature. All of those curves show that when the concentration is greater than 65%, the *COP* of the system is almost constant, that is because the heat of dissolution for unit mass of ammonia in different conditions is almost equal to each other. If the compression ratio is high, indicating that the work input to the compressor is lager, the system *COP* decreased. It is worthy to note that as the heat sink temperature is 65℃， if the heat source temperature is higher than 30℃, the *COP* is always higher than 4.0.

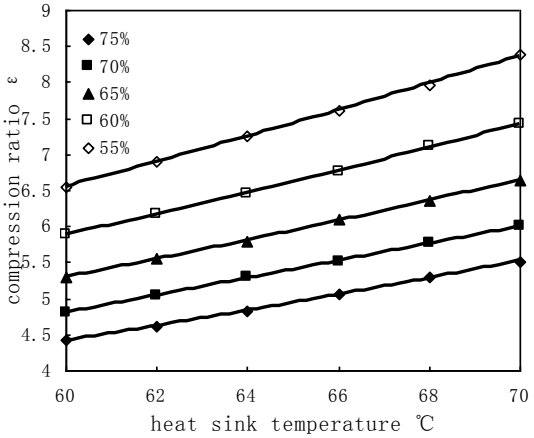

Fig. 9 The changes of ε along with heat sink temperature at different concentrations (heat source temperature T_{12}=30℃)

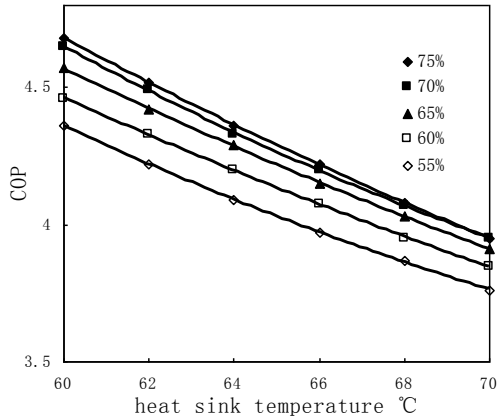

Fig. 10 The changes of *COP* along with heat sink temperature at different concentrations (heat source temperature T_{12}=30 ℃)

The dependence of compression ratio on heat sink temperature (T_{12}) for different values of concentration is shown in Fig. 9. The lower the concentration the higher the compression ratio, which means there is more power input to the system. For the different concentration the *COP* changes along with the heat sink temperature (T_{12}), as shown in Fig. 10. The *COP* changes sharply with the heat sink temperature. From the space between the curves, higher concentration can get higher *COP*, but the influence is diminishing with the increase of concentration. When the concentration is greater than 70%, the *COP* value almost does not change with the concentration, indicating that there should be an optimal concentration value for this system. According the analysis above the optimal value of solution concentration is around 65%.

5. CONCLUSIONS

A specialized numerical model for the generator and a model for the CAHP system using ammonia-water as the working fluid have been studied. The following conclusions can be drawn from the present study:

1) The maximum over all heat transfer coefficient of the out-tube falling film generator can be obtained in an optimum spray density of around 0.15 $kg \cdot m^{-1} \cdot s^{-1}$.

2) The concentration and heat source temperature can have the large effect on the performance of the generator at the low-temperature condition, and when the concentration is 65%, it can get a high concentration difference about 10%.

3) COP increases with the increase in concentration. There also exists an optimum concentration value of around 65%.

4) The models indicate that the out-tube falling film generator is appropriate for the CAHP system, when the system operating with a high heat sink temperature between 65 and 75℃, and a low heat source temperature from 30 to 40℃, the *COP* is above 4.

ACKNOWLEDGMENT

This work was financially supported by National Key Technology R&D Program in China (No. 2012BAB12B01)

NOMENCLATURE

COP the coefficient of performance

h enthalpy

δ film thickness

v velocity of y direction

u velocity of x direction

ξ solution concentration

λ coefficient of heat conductivity

ρ density

m mass flow

P pressure

ε compression ratio

U_g heat transfer coefficient of generator

V volume flow

η_{is} isentropic efficiency

f cycle ratio

T temperature

D_o outside diameter

D_i inner diameter

Γ inlet spray density

Subscripts

1~12 condition points of fig.1

0 initial state

a absorber

g generator

w water

REFERENCES

Rameshkumar, A., Udayakumar, M., and Saravanan, R.: Heat transfer studies on a GAXCAC(generator-absorber-exchange absorption compression) cooler. *Appl. Energy*, 86, (2009): 2056-2064

Bourouis, M., Nogues, M., Boer, D. and Coronas, A.: Industrial heat recovery by absorption/compression heat pump using TFE-H_2O-TEGDME working mixture. *Appl. Therm. Eng*., 20, (2000): 355-369

Fukuta, M., Yanagisawa, T., Iwata, H., and Tada, K.: Performance of compression/absorption hybrid refrigeration cycle with propane/mineral oil combination. *Int. J. Refrig.,* 25, (2002): 907-915

Satapathy, P. K.: Exergy analysis of a compression-absorption system for heating and cooling applications. *Int. J. Energ. Res.,* 32, (2008): 1266-1278

Stokar, M., and Trepp, C.: Compression heat pump with solution circuit part1:design and experimental results. *Int. J. Refrig*., 10, (1986): 87-96

Stokar, M.: Compression heat pump with solution circuit part2: Sensitivity analysis of construction and control parameters. *Int. J. Refrig*., 10, (1987): 134-142

Eckhard, A. G.: Current status of absorption/compression cycle technology. *Ashare Transactions symposia*, (1997): 361-373

Ventas, R., Lecuona, A., Zacarias, A., and Venegas, M.: Ammonia-lithium nitrate absorption chiller with an integrated low-pressure compression booster cycle for low driving temperatures. *Appl.Therm. Eng*., 30, (2010):1351-1359

Hulten, M., and Berntsson, T.: The compression/absorption cycle-influence of same major parameters on COP and a comparison with the compression cycle. *Int. J. Refrig*., 22, (1999): 91-106

Hulten, M., and Berntsson, T.: The compression/absorption heat pump cycle-conceptual design improvements and comparison with the compression cycle. *Int. J. Refrig*., 25, (2002): 487-497

Chun, K. R. and Seban, R.A.: Heat transfer to evaporating liquid film, *ASME J. Heat Transfer*, (1971): 391–396

Tyagi, S.T., Kim, M. S., Park, S.R., and Anand, S.: Second law based performance of modified VAC hybrid heat pump system using NH_3-H_2O as the working fluid. *Indian J. Pure. Ap. Phy*., (2010): 212-219

Xu, S. M.: Derivation of NH_3-H_2O thermodynamic parameters expression and programming. *Fluid Machinery*, 23, (1995): 55-59